Supplementary material

Theoretical limits for negative elastic moduli in sub-acoustic lattice materials

T. Mukhopadhyay[a,*], S. Adhikari[b], A. Alu[c]

[a] *Department of Engineering Science, University of Oxford, Oxford, UK*
[b] *College of Engineering, Swansea University, Swansea, UK*
[c] *Advanced Science Research Center, City University of New York, New York, USA*

Abstract

To obtain the closed-form theoretical limits of natural frequency, beyond which negative elastic moduli can be realized in lattice materials, the frequency-dependent expressions for elastic moduli of lattices are needed. On the basis of a unit cell based approach, closed-form expressions for the complex elastic moduli are derived as a function of frequency by employing the dynamic stiffness matrix of a damped beam element. In this supplementary material, we have provided the derivation of the dynamic stiffness matrix for a single beam element first. Thereby, the derivation of closed-form expressions of the frequency-dependent elastic moduli of lattice materials are presented. The theoretical limits of frequency to obtain negative elastic moduli are obtained based on their respective closed-form expressions. Here we also show results for validation of the proposed dynamic stiffness based framework, based on which the theoretical limits are derived.

Contents

*Corresponding author: Tanmoy Mukhopadhyay
Email address: tanmoy.mukhopadhyay@eng.ox.ac.uk (T. Mukhopadhyay)

1. Dynamic stiffness approach

1.1. Equation of motion

Dynamic motion of the overall cellular structure corresponds to vibration of individual beams which constitute each hexagonal unit cells. A pictorial depiction of the beam is shown in figure 1(c) of the main manuscript. One honeycomb unit cell under dynamic environment is shown in figure 1(b) of the main manuscript, wherein a vibrating mode of each constituent members is symbolically shown. If external forces are applied to such vibrating honeycomb, the members will deform following a different rule. Thus the effective elastic moduli of the entire lattice will be different from conventional static elastic moduli. Aim of the present article is to capture the effect of vibration in the effective elastic moduli of hexagonal lattices based on dynamic stiffness method [9, 16]. The dynamic stiffness matrix of a single beam element is derived first (section 1); thereby the expressions of frequency dependent elastic moduli of the lattice metamaterial are developed based on the elements of the dynamic stiffness matrix of a single beam (section 2).

The equation of motion of free vibration of a damped beam can be expressed as

$$EI\frac{\partial^4 V(x,t)}{\partial x^4} + \widehat{c}_1\frac{\partial^5 V(x,t)}{\partial x^4 \partial t} + m\frac{\partial^2 V(x,t)}{\partial t^2} + \widehat{c}_2\frac{\partial V(x,t)}{\partial t} = 0 \tag{1}$$

It is assumed that the behaviour of the beam follows the Euler-Bernoulli hypotheses. In the above equation EI is the bending rigidity, m is mass per unit length, $\widehat{c}_1$ is the strain-rate-dependent viscous damping coefficient, $\widehat{c}_2$ is the velocity-dependent viscous damping coefficient and $V(x,t)$ is the transverse displacement. The length of the beam is assumed to be L. Considering a harmonic motion with frequency ω we have

$$V(x,t) = v(x)\exp\left[\mathrm{i}\omega t\right] \tag{2}$$

where $\mathrm{i} = \sqrt{-1}$. Substituting this in the beam equation (1) one obtains

$$EI\frac{\mathrm{d}^4 v}{\mathrm{d}x^4} + \mathrm{i}\omega\widehat{c}_1\frac{\mathrm{d}^4 v}{\mathrm{d}x^4} - m\omega^2 v + \mathrm{i}\omega\widehat{c}_2 v = 0 \tag{3}$$

$$\text{or} \quad \frac{\mathrm{d}^4 v}{\mathrm{d}x^4} - b^4 v = 0 \tag{4}$$

where

$$b^4 = \frac{m\omega^2 - \mathrm{i}\omega\widehat{c}_2}{EI + \mathrm{i}\omega\widehat{c}_1} \tag{5}$$

Following the damping convention in dynamic analysis as in [18], we consider stiffness and mass proportional damping. Therefore, we express the damping constants as

$$\widehat{c}_1 = \zeta_k(EI) \quad \text{and} \quad \widehat{c}_2 = \zeta_m(m) \tag{6}$$

where ζ_k and ζ_m are stiffness and mass proportional damping factors. Substituting these, from Eq. (5) we have

$$b^4 = \frac{m\omega^2\left(1 - \mathrm{i}\zeta_m/\omega\right)}{EI\left(1 + \mathrm{i}\omega\zeta_k\right)} \tag{7}$$

The constant b is in general a complex number for any physically realistic damping values. The effect of mass proportional damping factor ζ_m linearly decreases with higher frequency whereas the effect of stiffness proportional damping factor ζ_k linearly increases with higher frequency. To obtain the characteristic equation, we consider

$$v(x) = \exp\left[\lambda x\right] \tag{8}$$

Substituting this in Eq. (4) one obtains

$$\lambda^4 - b^4 = 0 \tag{9}$$

$$\text{or} \quad \lambda = \mathrm{i}b, -\mathrm{i}b,\ b, -b \tag{10}$$

Next we use these solutions to obtain the dynamic shape functions of the beam.

1.2. Frequency dependent shape functions

For classical (static) finite element analysis of beams, cubic polynomials are used as shape functions (see for example [20]). Here we aim to incorporate frequency dependent dynamic shape functions, as used with the framework of the dynamic finite element method. The dynamic finite element method belongs to the general class of spectral methods for linear dynamical systems [9]. This approach, or approaches very similar to this, is known by various names such as the dynamic stiffness method [1–7, 10, 11, 17, 19], spectral finite element method [9, 13] and dynamic finite element method [14, 15].

The dynamic shape functions are obtained such that the equation of dynamic equilibrium is satisfied exactly at all points within the element. Similar to the classical finite element method, assume that the frequency-dependent displacement within an element is interpolated from the nodal displacements as

$$v(x,\omega) = \mathbf{N}^T(x,\omega)\widehat{\mathbf{v}}(\omega) \tag{11}$$

Here $\widehat{\mathbf{v}}(\omega) \in \mathbb{C}^n$ is the nodal displacement vector $\mathbf{N}(x,\omega) \in \mathbb{C}^n$ is the vector of frequency-dependent shape functions and $n = 4$ is the number of the nodal degrees-of-freedom. Suppose the $s_j(x,\omega) \in \mathbb{C}, j = 1, \cdots, 4$

are the basis functions which exactly satisfy Eq. (4). It can be shown that the shape function vector can be expressed as

$$\mathbf{N}(x,\omega) = \mathbf{\Gamma}(\omega)\mathbf{s}(x,\omega) \tag{12}$$

where the vector $\mathbf{s}(x,\omega) = \{s_j(x,\omega)\}^T, \forall\, j = 1,\cdots,4$ and the complex matrix $\mathbf{\Gamma}(\omega) \in \mathbb{C}^{4\times 4}$ depends on the boundary conditions. The elements of $\mathbf{s}(x,\omega)$ constitutes $\exp[\lambda_j x]$ where the values of λ_j are obtained from the solution of the characteristics equation as given in Eq. (10). An element for the damped beam under bending vibration is shown in figure 1(c) of the main manuscript. The degrees-of-freedom for each nodal point include a vertical and a rotational degrees-of-freedom.

In view of the solutions in Eq. (10), the displacement field with the element can be expressed by a linear combination of the basic functions $e^{-\mathrm{i}bx}, e^{\mathrm{i}bx}, e^{bx}$ and e^{-bx} so that in our notations $\mathbf{s}(x,\omega) = \left\{e^{-\mathrm{i}bx}, e^{\mathrm{i}bx}, e^{bx}, e^{-bx}\right\}^T$. We can also express $\mathbf{s}(x,\omega)$ in terms of trigonometric functions. Considering $e^{\pm\mathrm{i}bx} = \cos(bx) \pm \mathrm{i}\sin(bx)$ and $e^{\pm bx} = \cosh(bx) \pm \mathrm{i}\sinh(bx)$, the vector $\mathbf{s}(x,\omega)$ can be alternatively expressed as

$$\mathbf{s}(x,\omega) = \begin{Bmatrix} \sin(bx) \\ \cos(bx) \\ \sinh(bx) \\ \cosh(bx) \end{Bmatrix} \in \mathbb{C}^4 \tag{13}$$

For steady-state dynamic response, the displacement field within the element can be expressed as

$$v(x) = \mathbf{s}(x,\omega)^T\mathbf{v} \tag{14}$$

where $\mathbf{v} \in \mathbb{C}^4$ is the vector of constants to be determined from the boundary conditions.

The relationship between the shape functions and the boundary conditions can be represented as in Table 1, where boundary conditions in each column give rise to the corresponding shape function. Writing

Table 1: The relationship between the boundary conditions and the shape functions for the bending vibration of beams.

	$N_1(x,\omega)$	$N_2(x,\omega)$	$N_3(x,\omega)$	$N_4(x,\omega)$
$y(0)$	1	0	0	0
$\dfrac{\mathrm{d}y}{\mathrm{d}x}(0)$	0	1	0	0
$y(L)$	0	0	1	0
$\dfrac{\mathrm{d}y}{\mathrm{d}x}(L)$	0	0	0	1

Eq. (14) for the above four sets of boundary conditions, one obtains

$$[\mathbf{R}]\left[\mathbf{y}^1, \mathbf{y}^2, \mathbf{y}^3, \mathbf{y}^4\right] = \mathbf{I} \tag{15}$$

where

$$\mathbf{R} = \begin{bmatrix} s_1(0) & s_2(0) & s_3(0) & s_4(0) \\ \frac{\mathrm{d}s_1}{\mathrm{d}x}(0) & \frac{\mathrm{d}s_2}{\mathrm{d}x}(0) & \frac{\mathrm{d}s_3}{\mathrm{d}x}(0) & \frac{\mathrm{d}s_4}{\mathrm{d}x}(0) \\ s_1(L) & s_2(L) & s_3(L) & s_4(L) \\ \frac{\mathrm{d}s_1}{\mathrm{d}x}(L) & \frac{\mathrm{d}s_2}{\mathrm{d}x}(L) & \frac{\mathrm{d}s_3}{\mathrm{d}x}(L) & \frac{\mathrm{d}s_4}{\mathrm{d}x}(L) \end{bmatrix} \tag{16}$$

and $\mathbf{y}^k$ is the vector of constants giving rise to the kth shape function. In view of the boundary conditions represented in Table 1 and equation (15), the shape functions for bending vibration can be shown to be given by Eq. (12) where

$$\mathbf{\Gamma}(\omega) = \left[\mathbf{y}^1, \mathbf{y}^2, \mathbf{y}^3, \mathbf{y}^4\right]^T = \left[\mathbf{R}^{-1}\right]^T \tag{17}$$

By obtaining the matrix $\mathbf{\Gamma}(\omega)$ from the above equation, the shape function vector can be obtained from Eq. (12). After some algebraic simplifications, we have represented the frequency dependent complex shape functions as

$$\begin{Bmatrix} N_1(x,\omega) \\ N_2(x,\omega) \\ N_3(x,\omega) \\ N_4(x,\omega) \end{Bmatrix} = \begin{bmatrix} \frac{1}{2}\frac{cS+Cs}{cC-1} & -\frac{1}{2}\frac{1+sS-cC}{cC-1} & -\frac{1}{2}\frac{cS+Cs}{cC-1} & \frac{1}{2}\frac{cC+sS-1}{cC-1} \\ \frac{1}{2}\frac{cC+sS-1}{b(cC-1)} & \frac{1}{2}\frac{-Cs+cS}{b(cC-1)} & -\frac{1}{2}\frac{1+sS-cC}{b(cC-1)} & -\frac{1}{2}\frac{-Cs+cS}{b(cC-1)} \\ -\frac{1}{2}\frac{S+s}{cC-1} & \frac{1}{2}\frac{C-c}{cC-1} & \frac{1}{2}\frac{S+s}{cC-1} & -\frac{1}{2}\frac{C-c}{cC-1} \\ \frac{1}{2}\frac{C-c}{b(cC-1)} & -\frac{1}{2}\frac{S-s}{b(cC-1)} & -\frac{1}{2}\frac{C-c}{b(cC-1)} & -\frac{1}{2}\frac{S-s}{b(cC-1)} \end{bmatrix} \begin{Bmatrix} \sin bx \\ \cos bx \\ \sinh bx \\ \cosh bx \end{Bmatrix} \tag{18}$$

where

$$C = \cosh(bL), \quad c = \cos(bL), \quad S = \sinh(bL) \quad \text{and} \quad s = \sin(bL) \tag{19}$$

and b is defined in (7).

1.3. Element dynamic stiffness matrix

The stiffness and mass matrices can be obtained following the conventional variational formulation [8]. The only difference is instead of classical cubic polynomials as the shape functions, frequency dependent shape functions in (18) should be used. It is convenient to define the dynamic stiffness matrix as

$$\mathbf{D}(\omega) = \mathbf{K}(\omega) - \omega^2\mathbf{M}(\omega) \tag{20}$$

so that the equation of dynamic equilibrium is

$$\mathbf{D}(\omega)\widehat{\mathbf{v}}(\omega) = \widehat{\mathbf{f}}(\omega) \tag{21}$$

In Eq. (20), the frequency-dependent stiffness and mass matrices can be obtained from

$$\mathbf{K}(\omega) = EI \int_0^L \frac{\mathrm{d}^2\mathbf{N}(x,\omega)}{\mathrm{d}x^2} \frac{\mathrm{d}^2\mathbf{N}^T(x,\omega)}{\mathrm{d}x^2} \mathrm{d}x \tag{22}$$

$$\text{and} \quad \mathbf{M}(\omega) = m \int_0^L \mathbf{N}(x,\omega)\mathbf{N}^T(x,\omega)\mathrm{d}x \tag{23}$$

After some algebraic simplifications it can be shown that the dynamic stiffness matrix is given by the following closed-form expression

$$\mathbf{D}(\omega) = \frac{EIb}{(cC-1)} \begin{bmatrix} -b^2(cS+Cs) & -sbS & b^2(S+s) & -b(C-c) \\ -sbS & -Cs+cS & b(C-c) & -S+s \\ b^2(S+s) & b(C-c) & -b^2(cS+Cs) & sbS \\ -b(C-c) & -S+s & sbS & -Cs+cS \end{bmatrix} \tag{24}$$

The elements of this matrix are frequency dependent complex quantities because b is a function of ω and the damping factors.

2. The derivation of frequency-dependent elastic moduli

Considering only the static deformation of a unit cell, [12] obtained the equivalent elastic moduli of the hexagonal cellular materials as

$$E_{1GA} = E\left(\frac{t}{l}\right)^3 \frac{\cos\theta}{(\frac{h}{l}+\sin\theta)\sin^2\theta} \tag{25}$$

$$E_{2GA} = E\left(\frac{t}{l}\right)^3 \frac{(\frac{h}{l}+\sin\theta)}{\cos^3\theta} \tag{26}$$

$$\nu_{12GA} = \frac{\cos^2\theta}{(\frac{h}{l}+\sin\theta)\sin\theta} \tag{27}$$

$$\nu_{21GA} = \frac{(\frac{h}{l}+\sin\theta)\sin\theta}{\cos^2\theta} \tag{28}$$

$$\text{and} \quad G_{12GA} = E\left(\frac{t}{l}\right)^3 \frac{\left(\frac{h}{l}+\sin\theta\right)}{\left(\frac{h}{l}\right)^2(1+2\frac{h}{l})\cos\theta} \tag{29}$$

where $(.)_{GA}$ represents the expressions of elastic moduli of regular hexagonal honeycombs. The cell walls are treated as beams of thickness t and Young's modulus E. The quantities l and h are the lengths of inclined cell walls having inclination angle θ and the vertical cell walls respectively. A key interest in this section is to obtain equivalent expressions when harmonic forcing is considered. The central idea behind the proposed derivation is to exploit the physical interpretation of the elements of the dynamic stiffness matrix obtained in the previous section.

Using equation (24), the analytical expressions of the frequency dependent in-plane elastic moduli will be obtained. For the purpose of deriving the expressions, the dynamic stiffness matrix is written in the following form for notational convenience

$$\mathbf{D}(\omega) = \begin{bmatrix} D_{11} & D_{12} & D_{13} & D_{14} \\ D_{21} & D_{22} & D_{23} & D_{24} \\ D_{31} & D_{32} & D_{33} & D_{34} \\ D_{41} & D_{42} & D_{43} & D_{44} \end{bmatrix} \tag{30}$$

where D_{ij} $(i, j = 1, 2, 3, 4)$ has the expressions corresponding to the terms of equation (24).

2.1. Derivation of Young's modulus E_1

One cell wall is considered for deriving the expression of the Young's modulus E_1 under the application of stress in direction - 1 as shown in figure 1(a) [12]. In the free body diagram of the slant member in figure 1(a), the rotational displacements of both ends and the bending displacement of one end is considered as zero. To satisfy the equilibrium of forces in direction -2, the force C is needed to be zero. Thus from the dynamic stiffness matrix presented in equation (30), the bending deflection of one end of the slant member with respect to the other end can be written as

$$\delta = \frac{P \sin\theta}{D_{33}} \tag{31}$$

where $P = \sigma_1(h + l\sin\theta)\bar{b}$ (geometric dimensions of a single honeycomb cell is shown in figure 1(b) of the main manuscript. $\bar{b}$ is the width of the beam i.e. thickness of the honeycomb sheet). The component of δ in direction - 1 is $\delta \sin\theta$. Thus the strain component in direction - 1 due to applied stress in the same direction can be expressed as

$$\begin{aligned} \epsilon_{11} &= \frac{\delta \sin\theta}{l\cos\theta} \\ &= \frac{\sigma_1(h + l\sin\theta)\bar{b}\sin^2\theta}{D_{33} l\cos\theta} \end{aligned} \tag{32}$$

The expression of D_{33} is given in equation (24) and (30). Replacing the expression for D_{33} and $I = \dfrac{\bar{b}t^3}{12}$, the Young's modulus E_1 can be obtained as

$$\begin{aligned} E_1(\omega) = \frac{\sigma_1}{\epsilon_{11}} &= \frac{D_{33} l\cos\theta}{(h + l\sin\theta)\bar{b}\sin^2\theta} \\ &= \frac{Et^3 l\cos\theta b^3(\cos(bl)\sinh(bl) + \cosh(bl)\sin(bl))}{12(h + l\sin\theta)\sin^2\theta(1 - \cos(bl)\cosh(bl))} \end{aligned} \tag{33}$$

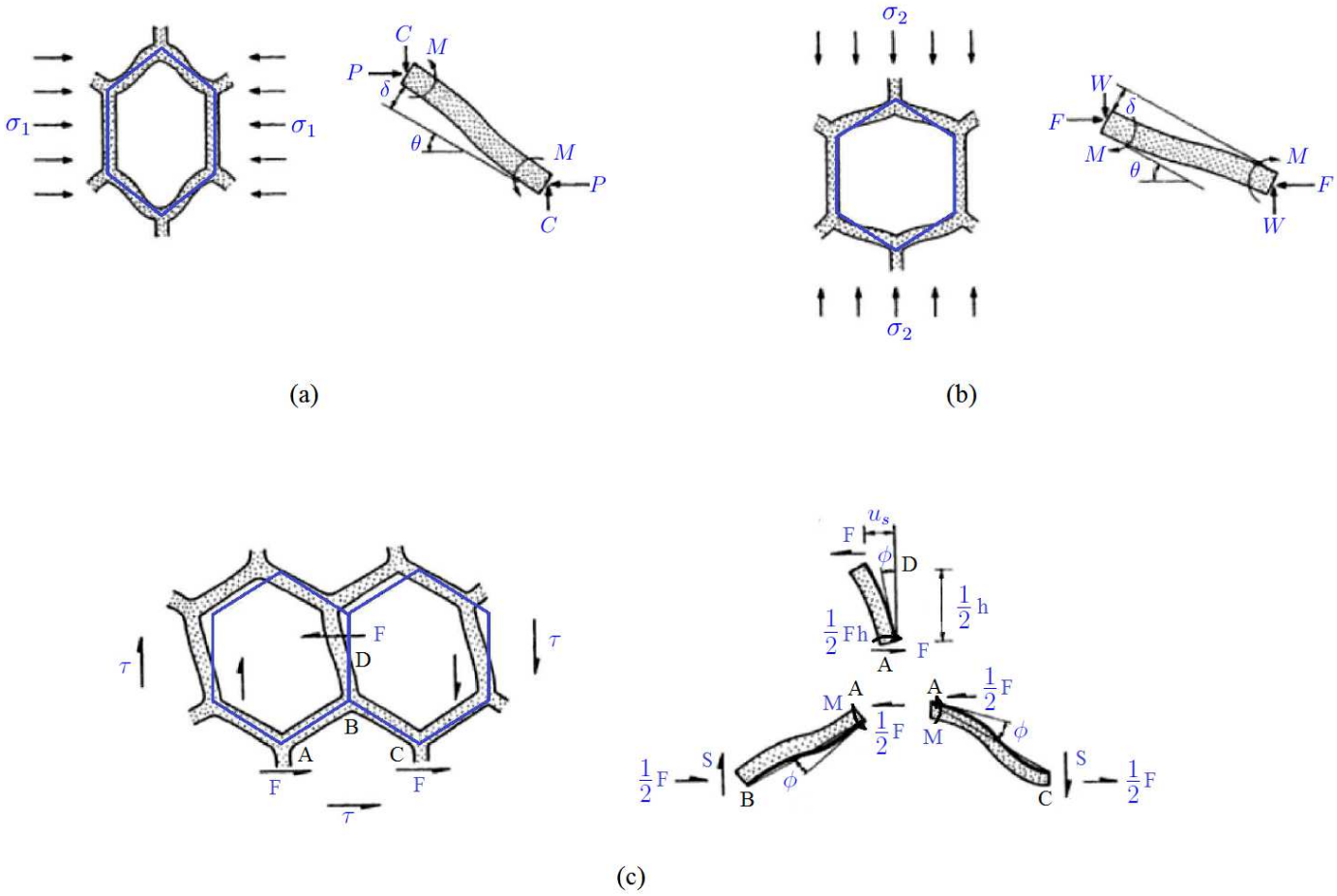

Figure 1: Deformed shapes and free body diagrams under the application of direct stresses and shear stress. The undeformed shapes of the hexagonal cell are indicated using blue colour for each of the loading conditions.

The expression of b is provided in equation (7). E is the intrinsic elastic modulus of the honeycomb material and t is the thickness of honeycomb wall.

2.2. Derivation of Young's modulus E_2

Similar to the derivation of E_1, the bending deformation of one end of the slant beam under the application of σ_2 (as shown in figure 1(b)) can be expressed as

$$\delta = \frac{W \cos\theta}{D_{33}} \tag{34}$$

where $W = \sigma_2 l\bar{b} \cos\theta$. The expression for strain component in direction - 2 due to application of stress in the same direction can be obtained as

$$\begin{aligned} \epsilon_{22} &= \frac{\delta \cos\theta}{(h + l\sin\theta)} \\ &= \frac{\sigma_2 l\bar{b} \cos^3\theta}{D_{33}(h + l\sin\theta)} \end{aligned} \tag{35}$$

Replacing the expression for D_{33} and $I = \dfrac{\bar{b}t^3}{12}$, the Young's modulus E_2 can be obtained as

$$\begin{aligned} E_2(\omega) = \frac{\sigma_2}{\epsilon_{22}} &= \frac{D_{33}(h + l\sin\theta)}{l\bar{b}\cos^3\theta} \\ &= \frac{Et^3(h + l\sin\theta)b^3\left(\cos(bl)\sinh(bl) + \cosh(bl)\sin(bl)\right)}{12l\cos^3\theta(1 - \cos(bl)\cosh(bl))} \end{aligned} \tag{36}$$

The expression of b is provided in equation (7), E is the intrinsic elastic modulus of the honeycomb material and t is the thickness of honeycomb wall as before.

2.3. Derivation of shear modulus G_{12}

For deriving the expression of G_{12}, two members of the honeycomb cell are needed to be considered (vertical member with length $\dfrac{h}{2}$ and a slant member with length l) as shown in figure 1(c). The points A, B and C will not have any relative movement due to symmetrical structure. The total shear deflection u_s consists of two components, bending deflection of the member BD and its deflection due to rotation of joint B.

It can be noted here that the elements of the dynamic stiffness matrix (refer to equation(30)) will be different for the vertical member and the slant member due to their different lengths. Using the stiffness components of the dynamic stiffness matrix (refer to equation (30)), the bending deformation of point D with respect to point B in direction - 1 can be obtained as

$$\delta_b = \frac{F}{\left(D^v_{33} - \dfrac{D^v_{34}D^v_{43}}{D^v_{44}}\right)} = \frac{F}{\left(D^v_{33} - \dfrac{(D^v_{34})^2}{D^v_{44}}\right)} \tag{37}$$

Here $F = 2\tau l\bar{b}\cos\theta$ and we make use of the symmetry of the elements of the dynamic stiffness matrix. The superscript v in the elements of the dynamic stiffness matrix is used to indicate the stiffness element corresponding to the vertical member.

From the free body diagram presented in figure 1(c),

$$M = \frac{Fh}{4} \tag{38}$$

On the basis of equation (30), deflection of the end B with respect to the end C due to application of moment M at the end B is given as

$$\delta_r = \frac{M}{-D^s_{43}} \tag{39}$$

Here the superscript s in D_{43} is used to indicate the stiffness element corresponding to the slant member and the negative arise due to the direction of the rotation as given in figure 1(c) of the main manuscript.

Thus the rotation of joint B can be expressed as

$$\begin{aligned}\phi &= \frac{\delta_r}{l} \\ &= -\frac{Fh}{4lD^s_{43}}\end{aligned} \tag{40}$$

Total shear deformation under the application of shear stress τ can be expressed as

$$\begin{aligned}u_s &= \frac{1}{2}\phi h + \delta_b \\ &= -\frac{Fh^2}{8lD^s_{43}} + \frac{F}{\left(D^v_{33} - \frac{(D^v_{34})^2}{D^v_{44}}\right)}\end{aligned} \tag{41}$$

The shear strain is given by

$$\begin{aligned}\gamma &= \frac{2u_s}{(h + l\sin\theta)} \\ &= \frac{F}{(h + l\sin\theta)}\left(-\frac{h^2}{4lD^s_{43}} + \frac{2}{\left(D^v_{33} - \frac{(D^v_{34})^2}{D^v_{44}}\right)}\right) \\ &= \frac{2\tau l\bar{b}\cos\theta}{(h + l\sin\theta)}\left(-\frac{h^2}{4lD^s_{43}} + \frac{2}{\left(D^v_{33} - \frac{(D^v_{34})^2}{D^v_{44}}\right)}\right)\end{aligned} \tag{42}$$

Replacing the expressions for the stiffness components from equation (24) and (30), the shear modulus can be obtained as

$$\begin{aligned}G_{12}(\omega) = \frac{\tau}{\gamma} &= \frac{(h + l\sin\theta)}{2l\bar{b}\cos\theta}\frac{1}{\left(-\frac{h^2}{4lD^s_{43}} + \frac{2}{\left(D^v_{33} - \frac{(D^v_{34})^2}{D^v_{44}}\right)}\right)} \\ &= \frac{(h + l\sin\theta)}{2l\bar{b}\cos\theta}\frac{4EIb^3\sin(bl)\sinh(bl)\left(1 + \cos(bh/2)\cosh(bh/2)\right)}{\begin{array}{r}h^2b\left(1 - \cos(bl)\cosh(bl)\right)\left(1 + \cos(bh/2)\cosh(bh/2)\right) \\ + 8l\sin(bl)\sinh(bl)\left(\cosh(bh/2)\sin(bh/2) - \sinh(bh/2)\cos(bh/2)\right)\end{array}} \\ &= \frac{Et^3(h + l\sin\theta)b^3\sin(bl)\sinh(bl)\left(1 + \cos(bh/2)\cosh(bh/2)\right)}{\begin{array}{l}6l\cos\theta\left[h^2b\left(1 - \cos(bl)\cosh(bl)\right)\left(1 + \cos(bh/2)\cosh(bh/2)\right)\right. \\ \quad \left. + 8l\sin(bl)\sinh(bl)\left(\cosh(bh/2)\sin(bh/2) - \sinh(bh/2)\cos(bh/2)\right)\right]\end{array}}\end{aligned} \tag{43}$$

The expression of the complex variable b is provided in equation (7).

2.4. Derivation of Poisson's ratios ν_{12} and ν_{21}

The strain components in direction - 1 and direction - 2 under the application of stress σ_1 are given by (refer to figure 1(a))

$$\epsilon_{11} = \frac{\delta\sin\theta}{l\cos\theta} \tag{44}$$

$$\epsilon_{21} = \frac{-\delta \cos\theta}{h + l\sin\theta} \tag{45}$$

Thus the Poisson's ratio for loading direction - 1 can be obtained as

$$\begin{aligned} \nu_{12} &= -\frac{\epsilon_{21}}{\epsilon_{11}} \\ &= \frac{l\cos^2\theta}{(h + l\sin\theta)\sin\theta} \end{aligned} \tag{46}$$

Similarly the Poisson's ratio for loading direction - 2 can be obtained as

$$\begin{aligned} \nu_{21} &= -\frac{\epsilon_{12}}{\epsilon_{22}} \\ &= \frac{(h + l\sin\theta)\sin\theta}{l\cos^2\theta} \end{aligned} \tag{47}$$

It can be noted that the in-plane Poisson's ratios (Equation 46 and 47) are not dependent on frequency and the expressions are same as the case of static deformation provided by [12].

3. Theoretical limits of frequency for negative elastic moduli

Expressions of the frequency-dependent elastic moduli, as derived in the preceding section, can be summarized as:

$$E_1(\omega) = \frac{D_{33} l\cos\theta}{(h + l\sin\theta)\bar{b}\sin^2\theta} = \frac{Et^3 l\cos\theta b^3(\cos(bl)\sinh(bl) + \cosh(bl)\sin(bl))}{12(h + l\sin\theta)\sin^2\theta(1 - \cos(bl)\cosh(bl))} \tag{48}$$

$$E_2(\omega) = \frac{D_{33}(h + l\sin\theta)}{l\bar{b}\cos^3\theta} = \frac{Et^3(h + l\sin\theta)b^3\left(\cos(bl)\sinh(bl) + \cosh(bl)\sin(bl)\right)}{12l\cos^3\theta(1 - \cos(bl)\cosh(bl))} \tag{49}$$

$$\begin{aligned} G_{12}(\omega) &= \frac{(h + l\sin\theta)}{2l\bar{b}\cos\theta} \frac{1}{\left(-\frac{h^2}{4lD^s_{43}} + \frac{2}{\left(D^v_{33} - \frac{(D^v_{34})^2}{D^v_{44}}\right)}\right)} \\ &= \frac{Et^3(h + l\sin\theta)b^3\sin(bl)\sinh(bl)\left(1 + \cos(bh/2)\cosh(bh/2)\right)}{6l\cos\theta\left[h^2 b\left(1 - \cos(bl)\cosh(bl)\right)\left(1 + \cos(bh/2)\cosh(bh/2)\right)\right.} \\ &\qquad \left. + 8l\sin(bl)\sinh(bl)\left(\cosh(bh/2)\sin(bh/2) - \sinh(bh/2)\cos(bh/2)\right)\right] \end{aligned} \tag{50}$$

It can be noted here that the expressions of E_1 and E_2 are proportional to the complex frequency-dependent element D_{33} of the $[\mathbf{D}(\omega)]$ matrix. Therefore, we study it's behaviour in the undamped limit to understand the if the real part of E_1 and E_2 can become negative. Assuming no damping in the system, the parameter b becomes

$$b^4 = \frac{m\omega^2}{EI} \tag{51}$$

Substituting this in the expression of D_{33} and expanding the expression by a Taylor series in the frequency parameter ω we have

$$D_{33} = 12\,\frac{EI}{l^3} - \frac{13}{35}\,m\,l\omega^2 - \frac{59}{161700}\,\frac{l^5m^2\omega^4}{EI} - \frac{551}{794593800}\,\frac{l^9m^3\omega^6}{EI^2} + \cdots \tag{52}$$

Note that coefficients of some higher order terms of ω are negative. We observe that D_{33} appears as a multiplicative term in the expressions of $E_1(\omega)$ and $E_2(\omega)$ in equations (48) and (49) and the other terms are positive. Therefore, near the vicinity of $\omega \approx 0$, there exists a frequency beyond where the effective elastic moduli of honeycomb will be negative. Retaining up to terms of order ω^4 in equation (52), the critical value of ω can be obtained by setting $D_{33} = 0$ as

$$\begin{aligned} D_{33} &\approx 12\,\frac{EI}{l^3} - \frac{13}{35}\,m\,l\omega^2 - \frac{59}{161700}\,\frac{l^5m^2\omega^4}{EI} = 0 \\ \text{or} \quad \omega^*_{E_1,E_2} &\approx 5.598\frac{1}{l^2}\sqrt{\frac{EI}{m}} \end{aligned} \tag{53}$$

Here, $\omega^*_{E_1,E_2}$ represents the fundamental inflection frequency, where the Young's moduli change sign from positive to negative. For lightly damped systems, beyond this frequency value, the equivalent Young's moduli E_1 and E_2 will be negative for the first time when viewed on the frequency axis. As the frequency increases, the Young's moduli will become positive and negative again. The significance of the fundamental inflection frequency derived in equation (53) is that it is the *lowest* frequency value beyond which the effective Young's modulus can become negative. Physically, negative Young's modulus means that when a force is applied at the inflection frequency, the direction of the steady-state dynamic response will be in the opposite direction to the applied forcing at the same frequency.

Unlike the case of Young's moduli, the frequency-dependent closed-form expression 50 for shear modulus shows a compound effect of multiple elements of the $[\mathbf{D}(\omega)]$ matrix. It is possible to obtain the expression of a tight bound for the frequency, beyond which the shear modulus becomes negative. For the shear modulus, the frequency dependent expression (50) can be extended in a Taylor series in ω about $\omega = 0$ as

$$\begin{aligned} G_{12}(\omega) = \frac{(h + l\sin\theta)}{2l\bar{b}\cos\theta}\Bigg[24\frac{EI}{h^2\,(2h+l)} - \frac{11}{420}\frac{m\,(9h^5+8l^5)\,\omega^2}{h^2\,(2h+l)^2} \\ -\frac{1}{46569600}\frac{m^2\,(55461h^9l - 191664h^5l^5 + 198912l^9h + 3111h^{10} + 14272l^{10})\,\omega^4}{EIh^2\,(2h+l)^3} + \cdots\Bigg] \end{aligned} \tag{54}$$

Considering only up to the second-order terms we can obtain the upper-bound of the frequency, beyond

which the G_{12} will be negative as

$$\begin{aligned} 24\frac{EI}{h^2\left(2h+l\right)} - \frac{11}{420}\frac{m\left(9h^5+8l^5\right)\omega^2}{h^2\left(2h+l\right)^2} &\approx 0 \\ \text{or} \quad \omega^*_{G_{12}} \lessapprox 30.2715\sqrt{\frac{1+2(h/l)}{8+9(h/l)^5}}\frac{1}{l^2}\sqrt{\frac{EI}{m}} & \end{aligned} \tag{55}$$

The lower bound is obtained by considering the numerator of G_{12} in equation (50) and setting it to zero. Expanding the numerator of G_{12} in a Taylor series in b we have

$$\frac{1}{1440}\,h^2l^3\left(2\,h+l\right)\left(32\,l^4+15\,h^4\right)b^4 - 2\,h^2l^3\left(2\,h+l\right) \approx 0 \tag{56}$$

Solving this equation for b one obtains

$$b \approx 2\,\frac{\sqrt{30}}{\sqrt[4]{160\,l^4+75\,h^4}} \tag{57}$$

Using the relationship of ω for the undamped case in equation (51) results in the following relationship

$$\omega^*_{G_{12}} \gtrapprox \frac{120}{\sqrt{160+75\left(h/l\right)^4}}\frac{1}{l^2}\sqrt{\frac{EI}{m}} \tag{58}$$

Combining equations (55) and (58) we obtain the following fundamental inequality regarding the frequency for negative value of G_{12}

$$\frac{120}{\sqrt{160+75\left(h/l\right)^4}}\frac{1}{l^2}\sqrt{\frac{EI}{m}} \leq \omega^*_{G_{12}} \leq 30.2715\sqrt{\frac{1+2(h/l)}{8+9(h/l)^5}}\frac{1}{l^2}\sqrt{\frac{EI}{m}} \tag{59}$$

Here, $\omega^*_{G_{12}}$ represents the fundamental inflection frequency for shear modulus, where the shear modulus changes sign. Unlike the equivalent expression for the Young's moduli E_1 and E_2 in equation (53), for the minimum frequency above which G_{12} becomes negative depends on the h/l ratio.

It can be noted that the derivation of the efficient closed-form limits (equations 53 and 59) have only been possible due to the proposed dynamic stiffness based approach to obtain the expressions for the elastic moduli in a vibrating environment.

4. Numerical validation of the dynamic stiffness based framework

For discussing the results concerning negative elastic moduli with a high degree of confidence, the dynamic stiffness based framework needs to be validated first. We have presented representative results for validation of the analytical expression for frequency dependent Young's modulus here.

Two different validations are presented in this section. To verify the validity of the derived expression of the dynamic stiffness matrix we compare the results with the conventional finite element method considering

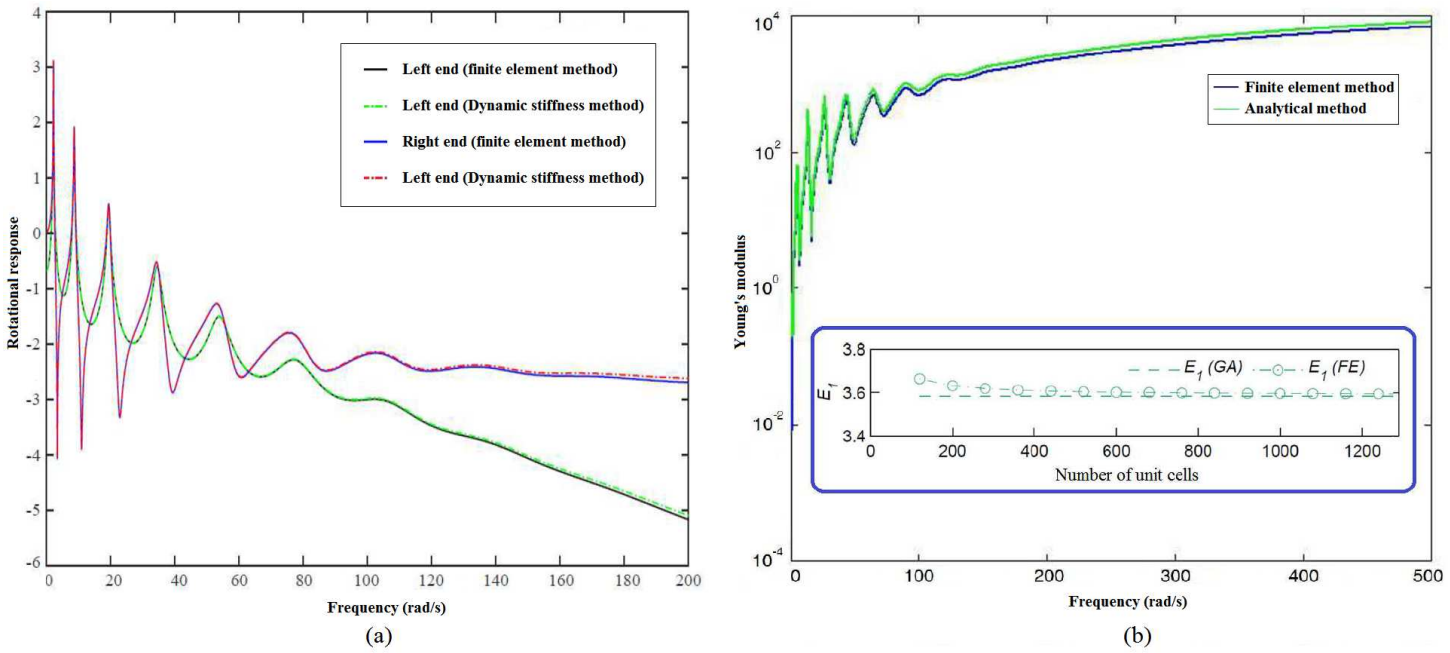

Figure 2: (a) Frequency-dependent responses of a pinned-pinned beam under the application of a unit moment at the right edge (b) Frequency dependent Young's modulus E_1 (with $h/l = 1$) of hexagonal lattices with $\theta = 30°$ and $\zeta_m = 0.05$ and $\zeta_k = 0.002$ (obtained using the analytical expressions and finite element method). A validation of the finite element (denoted by FE) model for static case (i.e. $\omega \to 0$) is shown in the inset along with a convergence study for the number of unit cells. The validation is presented with respect to the static analytical expression provided by [12] (denoted by GA).

a single beam element first. In figure 2(a) the responses of a pinned-pinned beam under the application of unit moment at the right edge are shown, wherein the rotational responses (radian) at the left and right edges are compared. The conventional finite element results are obtained by discretizing the beam into 100 elements and taking first 20 modes in the response calculations. The dynamic stiffness results are obtained using the closed-form expression obtained from only one element. The results match very well, confirming the validity and efficiency of applying the dynamic stiffness method.

After establishing that a single beam element using the dynamic stiffness matrix is capable to capture the dynamic behavior, we have validated the derived closed-form formulae for frequency-dependent elastic moduli with respect to the finite element approach. We have written a bespoke finite element code for the honeycomb lattice structure, where the stiffness matrix of each of the beam elements is used as the dynamic stiffness matrix. The finite element approach here involves transforming the element dynamic stiffness matrices for all beam elements into the global coordinate system, assembling them and applying the boundary conditions. The finite element model itself is validated with literature [12] in case of the static deformations (i.e. $\omega \to 0$) as shown in the inset of figure 2(b). The geometry, node numbers and nodal connectivity of the static case remains the same for the dynamic case. Therefore, the current validation

along with the dynamic validation for a single beam ensures the validation for the dynamic responses of the entire lattice. Figure 2(b) shows representative results obtained from the proposed closed-form expressions for the frequency dependent Young's modulus along with the results generated using finite element simulations. Numerical results obtained from the finite element approach for every frequency value is compared with the closed-form analytical expressions derived in the paper. Minor difference in the numerical values of the two results corresponding to a wide range of frequency corroborates the validity of the proposed expressions.

References

[1] Adhikari, S., Manohar, C. S., November 2000. Transient dynamics of stochastically parametered beams. ASCE Journal of Engineering Mechanics 126 (11), 1131–1140.

[2] Banerjee, J. R., 1989. Coupled bending torsional dynamic stiffness matrix for beam elements. International Journal for Numerical Methods in Engineering 28 (6), 1283–1298.

[3] Banerjee, J. R., 1997. Dynamic stiffness formulation for structural elements: A general approach. Computer and Structures 63 (1), 101–103.

[4] Banerjee, J. R., Fisher, S. A., 1992. Coupled bending torsional dynamic stiffness matrix for axially loaded beam elements. International Journal for Numerical Methods in Engineering 33 (4), 739–751.

[5] Banerjee, J. R., Williams, F. W., 1985. Exact bernoulli-euler dynamic stiffness matrix for a range of tapered beams. International Journal for Numerical Methods in Engineering 21 (12), 2289–2302.

[6] Banerjee, J. R., Williams, F. W., 1992. Coupled bending-torsional dynamic stiffness matrix for timoshenko beam elements. Computer and Structures 42 (3), 301–310.

[7] Banerjee, J. R., Williams, F. W., 1995. Free-vibration of composite beams - an exact method using symbolic computation. Journal of Aircraft 32 (3), 636–642.

[8] Dawe, D., 1984. Matrix and Finite Element Displacement Analysis of Structures. Oxford University Press, Oxford, UK.

[9] Doyle, J. F., 1989. Wave Propagation in Structures. Springer Verlag, New York.

[10] Ferguson, N. J., Pilkey, W. D., 1993. Literature review of variants of dynamic stiffness method, Part 1: The dynamic element method. The Shock and Vibration Digest 25 (2), 3–12.

[11] Ferguson, N. J., Pilkey, W. D., 1993. Literature review of variants of dynamic stiffness method, Part 2: Frequency-dependent matrix and other. The Shock and Vibration Digest 25 (4), 3–10.

[12] Gibson, L., Ashby, M. F., 1999. Cellular Solids Structure and Properties. Cambridge University Press, Cambridge, UK.

[13] Gopalakrishnan, S., Chakraborty, A., Mahapatra, D. R., 2007. Spectral Finite Element Method. Springer Verlag, New York.

[14] Hashemi, S. M., Richard, M. J., 2000. Free vibrational analysis of axially loaded bending-torsion coupled beams: a dynamic finite element. Computer and Structures 77 (6), 711–724.

[15] Hashemi, S. M., Richard, M. J., Dhatt, G., 1999. A new Dynamic Finite Element (DFE) formulation for lateral free vibrations of Euler-Bernoulli spinning beams using trigonometric shape functions. Journal of Sound and Vibration 220 (4), 601–624.

[16] Manohar, C., Adhikari, S., 1998. Dynamic stiffness of randomly parametered beams. Probabilistic Engineering Mechanics 13 (1), 39 – 51.

[17] Manohar, C. S., Adhikari, S., January 1998. Dynamic stiffness of randomly parametered beams. Probabilistic Engineering Mechanics 13 (1), 39–51.

[18] Meirovitch, L., 1997. Principles and Techniques of Vibrations. Prentice-Hall International, Inc., New Jersey.

[19] Paz, M., 1980. Structural Dynamics: Theory and Computation, 2nd Edition. Van Nostrand, Reinhold.

[20] Petyt, M., 1998. Introduction to Finite Element Vibration Analysis. Cambridge University Press, Cambridge, UK.